Submitted to small

DOI: 10.1002/smll.201002077

Exocytosis of mesoporous silica nanoparticles from mammalian cells: from asymmetric cell-to-cell transfer to protein harvesting

Igor I. Slowing, Juan L. Vivero-Escoto, Yannan Zhao, Kapil Kandel, Chorthip Peeraphatdit, Brian G. Trewyn* and Victor S.-Y. Lin†*

This work is dedicated to the memory of our dear colleague and friend Victor Shang-Yi Lin.

[*] Dr. I. I. Slowing
Program of Chemical and Biological Sciences
U.S. Department of Energy, Ames Laboratory
2756 Gilman Hall
Iowa State University
Ames, Iowa, 50011 (USA)
E-mail: islowing@iastate.edu

Dr. J.L. Vivero-Escoto
Department of Chemistry
Kenan Laboratories B521
The University of North Carolina at Chapel Hill
Chapel Hill, North Carolina, 27599 (USA)

[*] Dr. B. G. Trewyn, Mrs. Y. Zhao, Mr. K. Kandel, Mrs. C. Peeraphatdit
Department of Chemistry
1605 Gilman Hall
Iowa State University
Ames, Iowa, 50011 (USA)
E-mail: bgtrewyn@iastate.edu

† Prof. Dr. V. S.-Y. Lin (Deceased May 4, 2010)

Acknowledgements: This work was supported by the U.S. National Science Foundation (CHE-0809521), the authors thank BASF Co. for the kind donation of Pluronic P104 triblock co-polymer.

Supporting Information is available on the WWW under http://www.small-journal.com or from the author.

Keywords: Exocytosis; mesoporous silica nanoparticles; protein sequestration; drug delivery; cancer; enhanced permeability and retention

Mesoporous silica nanoparticles (MSNs) have raised considerable interest as vehicles for drug delivery because of their capacity to encapsulate large amounts of bioactive species and the ease with which their surface can be chemically modified.[1, 2] The versatile chemistry of MSNs has enabled their functionalization with several groups to render a variety of gated nanodevices, capable of controlling the loading and release of guest molecules in a stimuli-responsive fashion.[3-17] MSNs are readily endocytosed by animal and plant cells,[18-20] and their nanopatterned surface has proven to have a significant impact in their biocompatibility.[21, 22] All these properties have enabled the successful application of these materials to the delivery of drugs, genes and proteins into living cells, and more recently, into animal models of cancer.[1, 2, 8-10, 23-27] Since MSNs are readily taken up by a wide variety of cell types,[18-20] their use as vehicles for cell type-specific intracellular drug delivery might be conditioned to the incorporation of cell-targeting moieties.[28, 29] Cellular uptake, however, is not the only factor determining the selectivity of a drug delivery system: the relative abilities of the host cells to retain the nanoparticles also decide their ultimate fate. Herein we report an investigation on the relative abilities of healthy and cancerous cells to retain endocytosed MSNs, with the goal of further understanding the enhanced permeability and retention of nanoparticles recently observed in murine models of cancer.[27, 30, 44] In addition, the incorporation of magnetic nanoparticles into porous materials has been recently shown to enable their retrieval from liquid media.[31-33] Combining this with the known ability of MSNs to adsorb proteins,[34, 35] we explore the possibility of using the exocytosis of magnetically doped MSNs as a means for harvesting intracellular species.

Even if the *in vitro* endocytosis and the *in vivo* administration of MSNs have been systematically investigated, it is surprising to realize there are no studies on the exocytosis or cellular transport of these particles. This lack of reports could be related to the idea that MSNs may be too large for the cells to handle. In fact, a size retention factor has been recently suggested to account for the cellular withholding of aggregates of gold nanoparticles.[36, 37] However, even if MSNs are relatively large, their cellular uptake has been repeatedly proven to be energy-dependent, which suggests that cells employ their machinery to take these particles up.[20, 29, 38]

In contrast to MSNs, the exocytosis of non-porous nanoparticles has been studied several times. Most of the reports on the exocytosis of nanoparticles have been based on two main approaches: microscopic tracking, and measurement of intra- and extra-cellular particle concentrations.[36, 37, 39-43] These measurements have allowed the use of kinetic models to understand the dynamics of nanoparticle endo- and exocytosis.[40] Following these investigations, this study explores some of the consequences of nanoparticle exocytosis. On one hand it describes the role of exocytosis as a potential contributor to the enhanced permeability and retention of nanoparticles by cancer cells, which is known to take place mainly through hypervasculature,[27, 30, 44] and on the other it shows how the exocytosis of highly adsorbing nanoparticles can be used to harvest intracellular molecules. These new results place nanoparticle exocytosis in a context, demonstrating it is not only an interesting phenomenon, but it also plays an important role in biological processes, and has the potential to lead to valuable biotechnological applications.

Before investigating the processes resulting from the exocytosis of MSNs, it was necessary to establish the timeframe in which the ejection of the particles was most likely

to occur. To do so, we studied the uptake of fluorescein isothiocyanate-labeled MSNs (FITC-MSNs) by human umbilical vein endothelial cells (HUVECs) over time. These cells were chosen as models of healthy cells that surround diseased tissue in cancer. The cells were incubated in presence of the particles for increasing periods of time. The intracellular levels of FITC-MSNs were then monitored by flow cytometry, using the trypan blue exclusion method for quenching the fluorescence of extracellular particles.[45] The average fluorescence intensities of the cells suggested that the amounts of endocytosed FITC-MSNs increased gradually with time until reaching a plateau at approximately 2 h of contact (**Figure 1a**). This plateau can be considered as a state of equilibrium between the rates of endo- and exocytosis of the nanoparticles.[40] A similar behavior was observed when FITC-MSNs were incubated with human cervical cancer cells (HeLa) over the same period of time (**Figure 1b**).

Based on these results we proceeded to follow the exocytosis of FITC-MSNs from particle-saturated cells under fluorescence confocal microscope. After incubating HUVECs for 3 h in presence of FITC-MSNs, the particles were observed within the cell body at the same focal plane as the cell nucleus. Upon replenishing the culture with fresh media at 37°C, the exocytosis of FITC-MSNs was observed within 40 min. As can be observed in the upper set of frames of **Figure 2**, the fluorescent particles were initially co-localized with the cell body. During the first 15 to 20 min, the particles migrated gradually to the boundary of the cell membrane defining the shape of the cell (central set of frames). After some 40 min (lower set of frames of **Figure 2**) the labeled nanoparticles were found mainly in the extracellular space, demonstrating an active process of particle discharge. Interestingly, no exocytosis of FITC-MSNs was evident

when performing the same experiment with HeLa cells. Consistent with previous observations, endocytosis of the particles was less efficient when the cell growth medium contained serum than when it was free of serum.[46] Conversely, the presence of serum in the medium favored exocytosis, as previously reported for other nanoparticles.[42]

Based on these results we considered the possibility that MSNs exocytosed from one cell could be taken up by a neighboring cell. To evaluate this hypothesis we performed a series of cross-cell experiments (**Scheme 1**). In the first experiment, two cultures of HeLa cells were incubated for 3 h with fluorescently labeled MSNs: one using fluorescein isothiocyanate (FITC) and the other one using tetramethyl rhodamine isothiocyanate (TRITC) as a label. The cells were then washed with PBS, harvested by trypsinization, mixed and co-incubated for 20 h with serum-containing media at 37°C under 5.5% CO_2. The mixed cells were then washed, harvested and analyzed by flow cytometry. After setting gates using unlabeled cells, cells only loaded with FITC-MSNs, and cells only loaded with TRITC-MSNs as controls, it was possible to estimate that only a small fraction (12.6% ±1.6%) of the cells were FITC and TRITC positive (**Figure 3a**). We considered this result as a measure of the ability of the cells to exchange particles between each other. Examination under confocal microscope showed that indeed, the amount of double-labeled cells was very low (**Figure 3c**). When the same experiment was performed with HUVECs we observed a surprisingly large proportion of particle transfer between the cells containing FITC-MSNs and the ones containing TRITC-MSNs. The degree of transfer (89.6% ± 1.2%, **Figure 3b**) was seven times larger than the one observed with HeLa cells. Interestingly, the flow cytometry analysis of the mixture of HUVECs showed that instead of a single population with homogeneously distributed

amounts of both labeled MSNs, two different populations could be clearly identified: one having more FITC-MSNs than TRITC-MSNs, and another one with more TRITC-MSNs than FITC-MSNs. This high efficiency of intercellular MSN transfer in HUVECs was further confirmed by confocal fluorescence microscopy (**Figure 3d**).

We were further interested in determining if the observed differences between the MSN-transfer capabilities of HUVECs and HeLa cells could have implications in the distribution of MSNs in a co-culture of both types of cells. For that purpose we chose to label one cell type with a long-term cell tracer dye (Cell Trace™ Far Red DDAO-SE, Invitrogen) and treat the other cell type with FITC-MSNs. Since the cell tracer is not exchanged from cell to cell, it was possible to distinguish one cell type from the other throughout the experiment. As can be observed in **Figure 4a**, when HUVECs were stained with the tracer dye and HeLa cells were loaded with FITC-MSNs, very little particle transfer (7.5% ± 2.4%) could be observed. To the contrary, when HeLa cells were labeled with the tracer and HUVECs were loaded with the FITC-MSNs, the co-incubation of both cell types led to a large (74% ± 2.4%) amount of particle transfer (**Figure 4b**). It could be noted that, after transferring the FITC-MSNs to the HeLa cells, the fluorescence intensity of the HUVECs decreased, going from a relatively homogeneous distributed population (left plot) to a much wider distribution (right plot). These results suggest a unidirectional flow in the nanoparticle transfer between the two types of cell, which is consistent with the enhanced permeability and retention recently observed for porous silicon and silica nanoparticles in murine models of cancer.[27, 44]

It has been recently demonstrated that functionalized MSNs are able to capture nucleic acids inside of living cells.[47] Based on this observation, we hypothesized that

any endocytosed MSN should be able to sequester molecules found in its intracellular stage and keep them once exocytosed. Being that the case, it should be possible to detect the sequestered species by extraction from the recovered MSNs. Considering that MSNs are able to reversibly adsorb proteins,[48, 49] we decided to analyze the exocytosed nanoparticles in search of cellular proteins. To avoid any interference caused by proteins in the growth medium, we performed the exocytosis experiments in serum-free medium. MSNs with 10 nm wide pores were chosen to improve the adsorption of proteins (**Figure 5a**). To facilitate the isolation of the particles after exocytosis, we prepared superparamagnetic iron oxide nanoparticles in the interior of the pores of MSNs (**Figure 5a**), following a reported procedure.[50] Suspensions of magnetic-MSNs in serum-free medium (50 □g cm^{-3}) were added to cultures of HUVECs that were previously washed three times with serum-free medium. The cells were then incubated for different times ranging from 15 min to 4 h at 37°C and 5.5% CO_2. After the specific times, the supernatant was removed and transferred to another flask where the particles were isolated by means of a magnet and washed three times with PBS. The recovered magnetic-MSNs were then examined by transmission electron microscopy. The particles displayed several areas of low contrast material at their surface, and their pore structure was no longer visible (**Figure 5b**). These observations suggested the adsorption of organic molecules, possibly including proteins, to the particles. Thermogravimetric analysis showed that the percent of organic species adsorbed to the recovered MSNs increased with time up to a maximum of 6.5% after 4 h of incubation (**Figure 5c**). A sample of MSNs recovered after 4 h of incubation with HUVECs was then suspended in a solution of 10% glycerol, 5% 2-mercaptoethanol and 2% sodium dodecylsulfate, and

shaken overnight. Polyacrylamide electrophoretic analysis of the extract gave four bands (**Figure 5d**), which were later isolated, digested with trypsin, and subjected to tandem mass spectrometry analysis. A Mascot search of the resulting mass fingerprints in the MSDB, NCBInr and SwissProt databases identified sequences homologous to three proteins ($p<0.05$) for three of the four bands analyzed (**Table 1**).[51-54] The matching proteins, α-actinin-4, cytoplasmic actin-1 and annexin A2 are all associated with membrane and vesicular trafficking events. α-actinin-4 is an F-actin cross-linking protein that participates in receptor recycling and in the binding of actin to intracellular structures.[55, 56] Cytoplasmic actin is the main component of cytoskeleton and participates in intracellular transport.[57] Annexin A2 has been reported to link membrane phospholipids to actin and to play a key role in exocytosis.[58] These results strongly suggest that the particles were indeed endocytosed, adsorbed proteins at their intracellular stage, and were then exocytosed along with their cargoes. Furthermore, the observed association with actin is consistent with a recent report on the strong and dynamic interaction between submicron silica particles and the actin present in alveolar microvilli.[59]

In conclusion, the results obtained from the studies on the dynamics of cellular uptake of MSNs, cross-cell experiments, and protein sequestration by magnetic MSNs are all consistent with the hypothesis that mammalian cells can exocytose MSNs despite their relatively large size. We have demonstrated for the first time not only that exocytosis of MSNs takes place, but that there are significant differences between the abilities of different cells to retain or expel these nanoparticles, which lead to asymmetric cell-to-cell transfer of MSNs. We were also able to show that, due to their adsorptive

properties, MSNs have the ability to sequester and retrieve intracellular molecules. This ability could allow the future use of MSNs either as reporters of cellular processes or as nano-harvesters of cell-produced molecules.

Experimental Section

Synthesis of MSNs: MSNs were prepared by our previously reported method.[4] In brief, cetyltrimethylammonium bromide (CTAB, 1.02 g, 2.66 mmol) was dissolved in water (480 cm^3), followed by the addition of sodium hydroxide solution (2 M, 3.5 cm^3). The mixture was heated to 80 ºC with vigorous stirring, and then tetraethylorthosilicate (5.0 cm^3, 21.9 mmol) was added drop wise. The reaction mixture was stirred at this temperature for 2 h. The resulting solid was filtered, washed thoroughly with water and methanol and dried under vacuum for 20 h. The CTAB surfactant was removed by refluxing the material (1 g) in methanolic HCl (0.37 %, 100 cm^3). Fluorescent labeling was performed by reacting either fluorescein isothiocyanate (FITC) or tetramethyl rhodamine isothiocyanate (TRITC) with (3-aminopropyl)trimethoxysilane (APTMS) for 2 h in anhydrous dimethyl sulfoxide, and adding the resulting product to the initial CTAB reaction mixture. The products were characterized by x-ray diffraction in a Rigaku Ultima IV diffractometer, by nitrogen sorption analysis in a micromeritics tristar surface area and porosity analyzer using Brunauer-Emmett-Teller equation to calculate apparent surface area and pore volume and the Barret-Joyner-Halenda method to calculate pore size distribution, and by transmission electron microscopy of samples supported on copper grids in a Tecnai G2 F20 microscope operated at 200 kV.

Cellular uptake and exocytosis studies: Cells were seeded in six-well plates and incubated at 37°C under 5.5% CO_2 in the corresponding growth media (F-12K supplemented with heparin, endothelial growth factor and fetal bovine serum for HUVEC, and DMEM supplemented with penicillin, streptomycin, gentamicin, alanyl-glutamine and equine serum for HeLa). After 24 h incubation the growth media were replaced by suspensions of FITC-MSNs (50 and 100 μg cm^{-3}) in the corresponding growth media, and the cells were incubated for specific times (see main text). The suspensions were then discarded, the cells were harvested by trypsinization and resuspended in trypan blue solution for flow cytometry analysis. Flow cytometry was performed in a BD FACSCanto instrument. For confocal microscopy, glass cover slips were set in the bottom of the wells of the plates followed by addition of the cells. After cell attachment, the cells were incubated with FITC-MSNs for periods of time ranging from 1 to 4 h, the nuclei were then stained with Hoechst 33258 (blue) dye. The cells were imaged in a Leica SP5 X confocal system with Leica AFS Lite 2.1.0 imaging processing software under an oil-immersion 100x objective. For monitoring exocytosis the cells were not fixed and they were imaged using a heated stage (37 °C).

Synthesis of Magnetic MSNs: Large pore MSNs were prepared by modifying a literature procedure.[60] Pluronic P104 (courtesy of BASF, 7.0 g) was dissolved in a mixture of water (164 g) and aqueous HCl (4 M, 109 g) and kept stirring at 55 °C for 1 h. Tetramethyl orthosilicate (10.64 g) was quickly added into the solution at 55 °C. After continuous stirring for 24 h, the reaction mixture was moved to a teflon-lined, high-pressure autoclave for further hydrothermal treatment at 150 °C for 24 h. The product was isolated by filtration, washed with copious water and methanol, and dried at 80 °C in

air. The Pluronic P104 surfactant was removed from MSNs by calcination at 550 °C for 6 h. Magnetic MSNs were prepared following a literature procedure,[50] by adding a solution of Iron(III) nitrate in ethanol (1.26 g in 10 cm^{-3}) to large pore MSNs (0.5 g). The suspension was left to dry in air at 30 °C with constant stirring. The solid was then calcined in air at a heating rate of 10 °C min^{-1} to 300 °C. The resulting brownish powder was reduced by calcination in a constant flow of H_2 (1.67 cm^3 s^{-1}) at 300 °C for 5 h to give the resulting magnetic MSNs.

Cross-cell experiments: For each experiment two groups of cells (either both HUVEC or HeLa, or one HUVEC and the other one HeLa) were seeded in T-25 flasks and incubated for 24 h at 37°C and 5.5% CO_2. The growth medium was removed from each flask and replaced with a suspension of the labeled MSNs in growth media (FITC-MSNs in one flask, and TRITC-MSN or Cell Trace™ Far Red DDAO-SE from Invitrogen in the other), and incubated under the same conditions for further 3 h. The cells in each flask were then harvested by trypsinization and transferred into 6-well plates with fresh media (3 cm^{-3}). The cells were distributed in the wells in the following way: 3 wells with unlabeled cells, 3 wells with cells previously treated with FITC-MSNs, 3 wells with cells previously exposed either to TRITC-MSNs or Cell Trace dye (depending on the experiment), and 3 wells with a mixed suspension of the cells previously exposed to FITC-MSNs and the cells previously exposed to TRITC-MSNs or Cell Trace dye. The cells were incubated for further 20 hours at 37°C and 5.5% CO_2 and then harvested by trypsinization for flow cytometry analysis.

In addition, a well containing a cover slip in the bottom was also filled with the mixture of the cells exposed to FITC-MSNs and cells exposed to TRITC-MSNs and incubated

under the abovementioned conditions. After 24 h, the cells attached to the cover slips were treated with the nuclear stain Hoechst 33258, followed by fixation with 3.7% formaldehyde. Then the cells in the cover slips where mounted on microscope slides and imaged under a Leica SP5 X fluorescence confocal microscope with Leica AFS Lite 2.1.0 imaging processing software.

Protein sequestration study: HUVECs were seeded and incubated in T-75 flasks in the corresponding growth media for 2 to 3 days to attain the highest cell density possible. The media was then replaced by a suspension of magnetic MSNs in serum-free growth media (50 $\mu g\ cm^{-3}$, 50 cm^3) and incubated at 37°C and 5.5% CO_2 for specific times ranging from 15 min to 4 h. The flasks were then gently shaken and the supernatant was transferred to T-25 flasks with a one-inch diameter neodymium magnet taped to the exterior of a wall. After shaking the flasks the liquid was removed, and the magnet-immobilized particles were washed thrice with sterile phosphate buffered solution. For protein electrophoresis the particles were then suspended in a tris buffered solution (250 mm^3, 62 mM, pH 6.8) containing 10% glycerol, 5% 2-mercaptoethanol and 2% sodium dodecylsulfate, and shaken overnight at room temperature. The suspension was then heated to 95°C for 5 min and aliquots (30 mm^3) were loaded into the wells of a Tris-HCl polyacrylamide precast gel (10-20%, 10 wells, 50 mm^3 per well, Bio-Rad laboratories) and subjected to electrophoresis at 135 V for 75 min. The resulting gels were stained with coomassie-blue, destained with acetic-acid methanol and photographed. The resulting bands were cut from the gel, digested in trypsin and subjected to MALDI MS/MS analysis. The resulting MS/MS data were used to perform a database search using Mascot software.[51] For quantification of organics the recovered particles were

dried overnight under vacuum, and then subjected to thermogravimetric analysis in a TA Instruments 2950 Analyzer in air under atmospheric pressure. The heating rate was 2°C min^{-1} from 25°C to 650°C.

Received: ((will be filled in by the editorial staff))
Revised: ((will be filled in by the editorial staff))
Published online on ((will be filled in by the editorial staff))

Table of contents entry

The exocytosis of mesoporous silica nanoparticles (MSNs) from mammalian cells is demonstrated for the first time. The differences in the degree of exocytosis of MSNs between healthy and cancer cells are shown to be responsible for the asymmetric transfer of the particles between both cell types. The exocytosis of highly adsorbent magnetic MSNs proves to be useful as a means to harvest biomolecules from living cells.

Igor I. Slowing*, Juan L. Vivero-Escoto, Yannan Zhao, Kapil Kandel, Chorthip Peeraphatdit, Brian G. Trewyn* and Victor S.-Y. Lin†

*Corresponding Authors

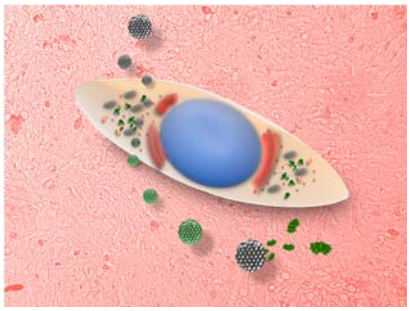

[1] J. Lu, M. Liong, J. I. Zink, F. Tamanoi, *Small* **2007**, *3*, 1341.
[2] I. I. Slowing, J. L. Vivero-Escoto, C.-W. Wu, V. S. Y. Lin, *Adv. Drug Deliv. Rev.* **2008**, *60*, 1278.
[3] N. K. Mal, M. Fujiwara, Y. Tanaka, *Nature* **2003**, *421*, 350.
[4] C.-Y. Lai, B. G. Trewyn, D. M. Jeftinija, K. Jeftinija, S. Xu, S. Jeftinija, V. S. Y. Lin, *J. Am. Chem. Soc.* **2003**, *125*, 4451.
[5] S. Angelos, Y.-W. Yang, K. Patel, J. F. Stoddart, J. I. Zink, *Angew. Chem. Int. Ed.* **2008**, *47*, 2222.
[6] J. Lu, E. Choi, F. Tamanoi, J. I. Zink, *Small* **2008**, *4*, 421.
[7] S. Angelos, N. M. Khashab, Y. W. Yang, A. Trabolsi, H. A. Khatib, J. F. Stoddart, J. I. Zink, *J. Am. Chem. Soc.* **2009**, *131*, 12912.
[8] R. Mortera, J. Vivero-Escoto, Slowing, II, E. Garrone, B. Onida, V. S. Y. Lin, *Chem. Commun.* **2009**, 3219.
[9] J. L. Vivero-Escoto, I. I. Slowing, C.-W. Wu, V. S.-Y. Lin, *J. Am. Chem. Soc.* **2009**, *131*, 3462.
[10] Y. Zhao, B. G. Trewyn, I. I. Slowing, V. S. Y. Lin, *J. Am. Chem. Soc.* **2009**, *131*, 8398.
[11] A. Bernardos, E. Aznar, M. D. Marcos, R. Martinez-Manez, F. Sancenon, J. Soto, J. M. Barat, P. Amoros, *Angew. Chem.-Int. Ed.* **2009**, *48*, 5884.
[12] E. Climent, A. Bernardos, R. Martinez-Manez, A. Maquieira, M. D. Marcos, N. Pastor-Navarro, R. Puchades, F. Sancenon, J. Soto, P. Amoros, *J. Am. Chem. Soc.* **2009**, *131*, 14075.
[13] Q. Yang, S. Wang, P. Fan, L. Wang, Y. Di, K. Lin, F.-S. Xiao, *Chem. Mater.* **2005**, *17*, 5999.
[14] Y. Yang, X. Yan, Y. Cui, Q. He, D. Li, A. Wang, J. Fei, J. Li, *J. Mater. Chem.* **2008**, *18*, 5731.
[15] C. Park, H. Kim, S. Kim, C. Kim, *J. Am. Chem. Soc.* **2009**, *131*, 16614.
[16] A. Schlossbauer, J. Kecht, T. Bein, *Angew. Chem.-Int. Ed.* **2009**, *48*, 3092.
[17] A. Schlossbauer, S. Warncke, P. Gramlich, J. Kecht, A. Manetto, T. Carell, T. Bein, *Angew. Chem. Int. Ed.* **2010**, *49*, 4734.
[18] D. R. Radu, C.-Y. Lai, K. Jeftinija, E. W. Rowe, S. Jeftinija, V. S. Y. Lin, *J. Am. Chem. Soc.* **2004**, *126*, 13216.
[19] F. Torney, B. G. Trewyn, V. S. Y. Lin, K. Wang, *Nature Nanotechnol.* **2007**, *2*, 295.
[20] D. M. Huang, Y. Hung, B. S. Ko, S. C. Hsu, W. H. Chen, C. L. Chien, C. P. Tsai, C. T. Kuo, J. C. Kang, C. S. Yang, C. Y. Mou, Y. C. Chen, *Faseb J.* **2005**, *19*, 2014.
[21] I. I. Slowing, C.-W. Wu, J. L. Vivero-Escoto, V. S. Y. Lin, *Small* **2009**, *5*, 57.
[22] Y.-S. Lin, C. L. Haynes, *J. Am. Chem. Soc.* **2010**, *132*, 4834.
[23] K. M. L. Taylor, J. S. Kim, W. J. Rieter, H. An, W. Lin, W. Lin, *J. Am. Chem. Soc.* **2008**, *130*, 2154.
[24] C.-H. Lee, S.-H. Cheng, Y.-J. Wang, Y.-C. Chen, N.-T. Chen, J. Souris, C.-T. Chen, C.-Y. Mou, C.-S. Yang, L.-W. Lo, *Adv. Funct. Mater.* **2009**, *19*, 215.
[25] I. I. Slowing, B. G. Trewyn, V. S. Y. Lin, *J. Am. Chem. Soc.* **2007**, *129*, 8845.
[26] J. Kim, H. S. Kim, N. Lee, T. Kim, H. Kim, T. Yu, I. C. Song, W. K. Moon, T. Hyeon, *Angew. Chem.-Int. Ed.* **2008**, *47*, 8438.

[27] J. Lu, M. Liong, Z. Li, J. I. Zink, F. Tamanoi, *Small* **2010**, *6*, 1794.
[28] C. P. Tsai, C. Y. Chen, Y. Hung, F. H. Chang, C. Y. Mou, *J. Mater. Chem.* **2009**, *19*, 5737.
[29] I. Slowing, B. G. Trewyn, V. S. Y. Lin, *J. Am. Chem. Soc.* **2006**, *128*, 14792.
[30] Y. Matsumura, H. Maeda, *Cancer Research* **1986**, *46*, 6387.
[31] L. Gu, J.-H. Park, K. H. Duong, E. Ruoslahti, M. J. Sailor, *Small* **2010**, *6*, 2546.
[32] J. R. Dorvee, M. J. Sailor, G. M. Miskelly, *Dalton Transactions* **2008**, 721.
[33] J. C. Thomas, C. Pacholski, M. J. Sailor, *Lab on a Chip* **2006**, *6*, 782.
[34] J. F. Díaz, K. J. Balkus, *J. Molec. Catal. B: Enzym.* **1996**, *2*, 115.
[35] S. Hudson, J. Cooney, E. Magner, *Angew. Chem.-Int. Ed.* **2008**, *47*, 8582.
[36] J. Nam, N. Won, H. Jin, H. Chung, S. Kim, *J. Am. Chem. Soc.* **2009**, *131*, 13639.
[37] B. D. Chithrani, W. C. W. Chan, *Nano Lett.* **2007**, *7*, 1542.
[38] J. Lu, M. Liong, S. Sherman, T. Xia, M. Kovochich, A. Nel, J. Zink, F. Tamanoi, *NanoBioTechnology* **2007**, *3*, 89.
[39] H. Jin, D. A. Heller, M. S. Strano, *Nano Lett.* **2008**, *8*, 1577.
[40] H. Jin, D. A. Heller, R. Sharma, M. S. Strano, *ACS Nano* **2009**, *3*, 149.
[41] I. Stayton, J. Winiarz, K. Shannon, Y. F. Ma, *Anal. Bioanal. Chem.* **2009**, *394*, 1595.
[42] J. Panyam, V. Labhasetwar, *Pharm. Res.* **2003**, *20*, 212.
[43] A. P. Alberola, J. O. Radler, *Biomater.* **2009**, *30*, 3766.
[44] J.-H. Park, L. Gu, G. von Maltzahn, E. Ruoslahti, S. N. Bhatia, M. J. Sailor, *Nat Mater* **2009**, *8*, 331.
[45] J. Hed, G. Hallden, S. G. O. Johansson, P. Larsson, *J. Immunol. Methods* **1987**, *101*, 119.
[46] X. L. Xing, X. X. He, J. F. Peng, K. M. Wang, W. H. Tan, *J. Nanosci. Nanotechnol.* **2005**, *5*, 1688.
[47] J. L. Vivero-Escoto, Slowing, II, V. S. Y. Lin, *Biomater.* **2010**, *31*, 1325.
[48] H. H. P. Yiu, C. H. Botting, N. P. Botting, P. A. Wright, *Phys. Chem. Chem. Phys.* **2001**, *3*, 2983.
[49] R. J. Tian, H. Zhang, M. L. Ye, X. G. Jiang, L. H. Hu, X. Li, X. H. Bao, H. F. Zou, *Angew. Chem.-Int. Ed.* **2007**, *46*, 962.
[50] H. H. P. Yiu, M. A. Keane, Z. A. D. Lethbridge, M. R. Lees, A. J. El Haj, J. Dobson, *Nanotechnol.* **2008**, *19*, 7.
[51] D. N. Perkins, D. J. C. Pappin, D. M. Creasy, J. S. Cottrell, *Electrophoresis* **1999**, *20*, 3551.
[52] K. D. Pruitt, T. Tatusova, D. R. Maglott, *Nucleic Acids Res.* **2005**, *33*, D501.
[53] A. Bairoch, U. Consortium, L. Bougueleret, S. Altairac, V. Amendolia, A. Auchincloss, G. Argoud-Puy, K. Axelsen, D. Baratin, M. C. Blatter, B. Boeckmann, J. Bolleman, L. Bollondi, E. Boutet, S. B. Quintaje, L. Breuza, A. Bridge, E. Decastro, L. Ciapina, D. Coral, E. Coudert, I. Cusin, G. Delbard, D. Dornevil, P. D. Roggli, S. Duvaud, A. Estreicher, L. Famiglietti, M. Feuermann, S. Gehant, N. Farriol-Mathis, S. Ferro, E. Gasteiger, A. Gateau, V. Gerritsen, A. Gos, N. Gruaz-Gumowski, U. Hinz, C. Hulo, N. Hulo, J. James, S. Jimenez, F. Jungo, V. Junker, T. Kappler, G. Keller, C. Lachaize, L. Lane-Guermonprez, P. Langendijk-Genevaux, V. Lara, P. Lemercier, V. Le Saux, D. Lieberherr, T. D. Lima, V. Mangold, X. Martin, P. Masson, K. Michoud, M.

Moinat, A. Morgat, A. Mottaz, S. Paesano, I. Pedruzzi, I. Phan, S. Pilbout, V. Pillet, S. Poux, M. Pozzato, N. Redaschi, S. Reynaud, C. Rivoire, B. Roechert, M. Schneider, C. Sigrist, K. Sonesson, S. Staehli, A. Stutz, S. Sundaram, M. Tognolli, L. Verbregue, A. L. Veuthey, L. Yip, L. Zuletta, R. Apweiler, Y. Alam-Faruque, R. Antunes, D. Barrell, D. Binns, L. Bower, P. Browne, W. M. Chan, E. Dimmer, R. Eberhardt, A. Fedotov, R. Foulger, J. Garavelli, R. Golin, A. Horne, R. Huntley, J. Jacobsen, M. Kleen, P. Kersey, K. Laiho, R. Leinonen, D. Legge, Q. Lin, M. Magrane, M. J. Martin, C. O'Donovan, S. Orchard, J. O'Rourke, S. Patient, M. Pruess, A. Sitnov, E. Stanley, M. Corbett, G. di Martino, M. Donnelly, J. Luo, P. van Rensburg, C. Wu, C. Arighi, L. Arminski, W. Barker, Y. X. Chen, Z. Z. Hu, H. K. Hua, H. Z. Huang, R. Mazumder, P. McGarvey, D. A. Natale, A. Nikolskaya, N. Petrova, B. E. Suzek, S. Vasudevan, C. R. Vinayaka, L. S. Yeh, J. Zhang, *Nucleic Acids Res.* **2009**, *37*, D169.

[54] in *MSDB: Mass Spectrometry protein sequence DataBase* *http://proteomics.leeds.ac.uk/bioinf/msdb.html*.

[55] Q. Yan, W. Sun, P. Kujala, Y. Lotfi, T. A. Vida, A. J. Bean, *Mol. Biol. Cell* **2005**, *16*, 2470.

[56] I. Talior-Volodarsky, V. K. Randhawa, H. Zaid, A. Klip, *J. Biol. Chem.* **2008**, *283*, 25115.

[57] T. D. Pollard, J. A. Cooper, *Science* **2009**, *326*, 1208.

[58] E. Morel, R. G. Parton, J. Gruenberg, *Dev. Cell* **2009**, *16*, 445.

[59] G. Orr, D. J. Panther, J. L. Phillips, B. J. Tarasevich, A. Dohnalkova, D. H. Hu, J. G. Teeguarden, J. G. Poundsl, *ACS Nano* **2007**, *1*, 463.

[60] P. Linton, V. Alfredsson, *Chem. Mater.* **2008**, *20*, 2878.

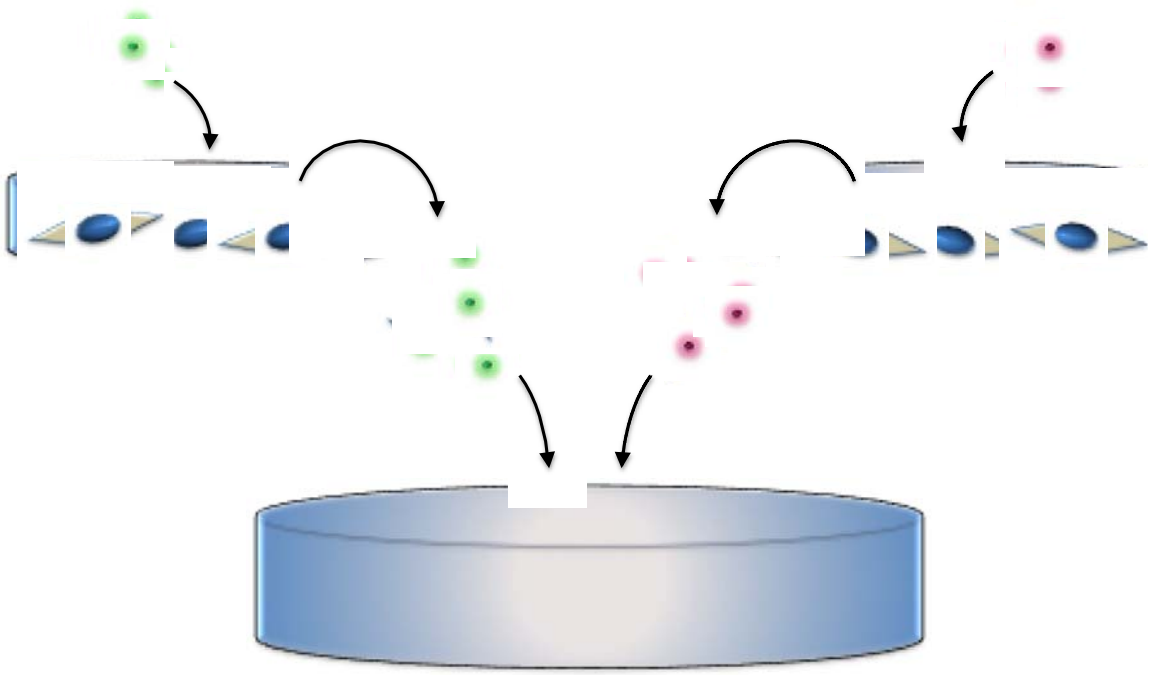

Scheme 1. Cross-cell experiments. Two cultures of cells were incubated separately, each with different labeled MSNs (FITC-MSNs one, TRITC-MSNs the other one). After uptake of the particles each culture was washed and harvested. Both cultures were then mixed and co-incubated to evaluate nanoparticle transfer between each other.

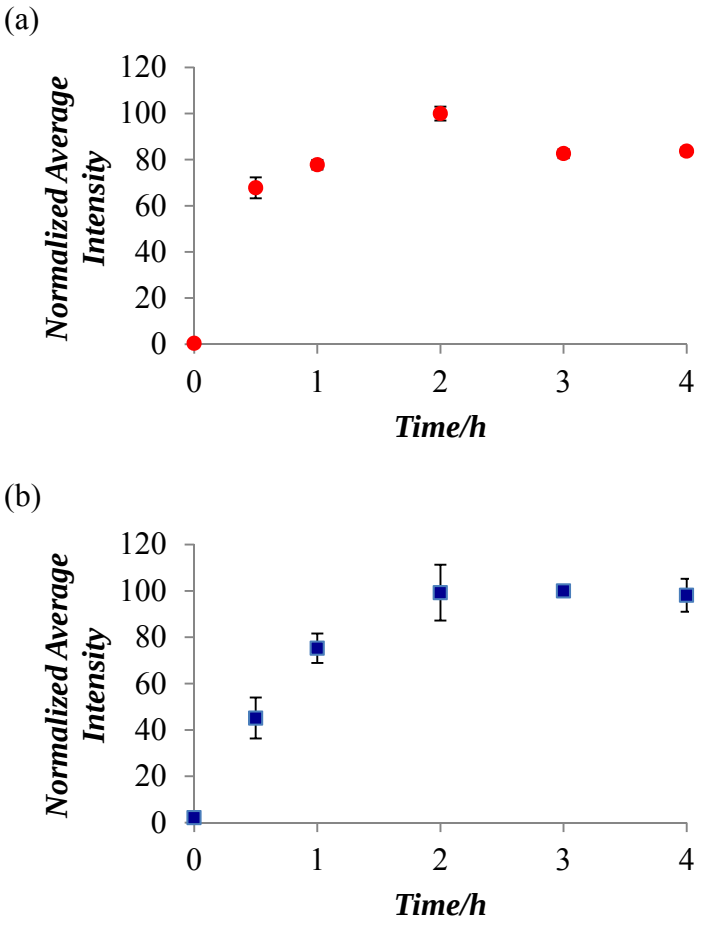

Figure 1. Changes in average fluorescence intensity of HUVEC (a) and HeLa (b) cells when incubated with suspensions of FITC-MSNs for different times. (Sample size $N = 3$).

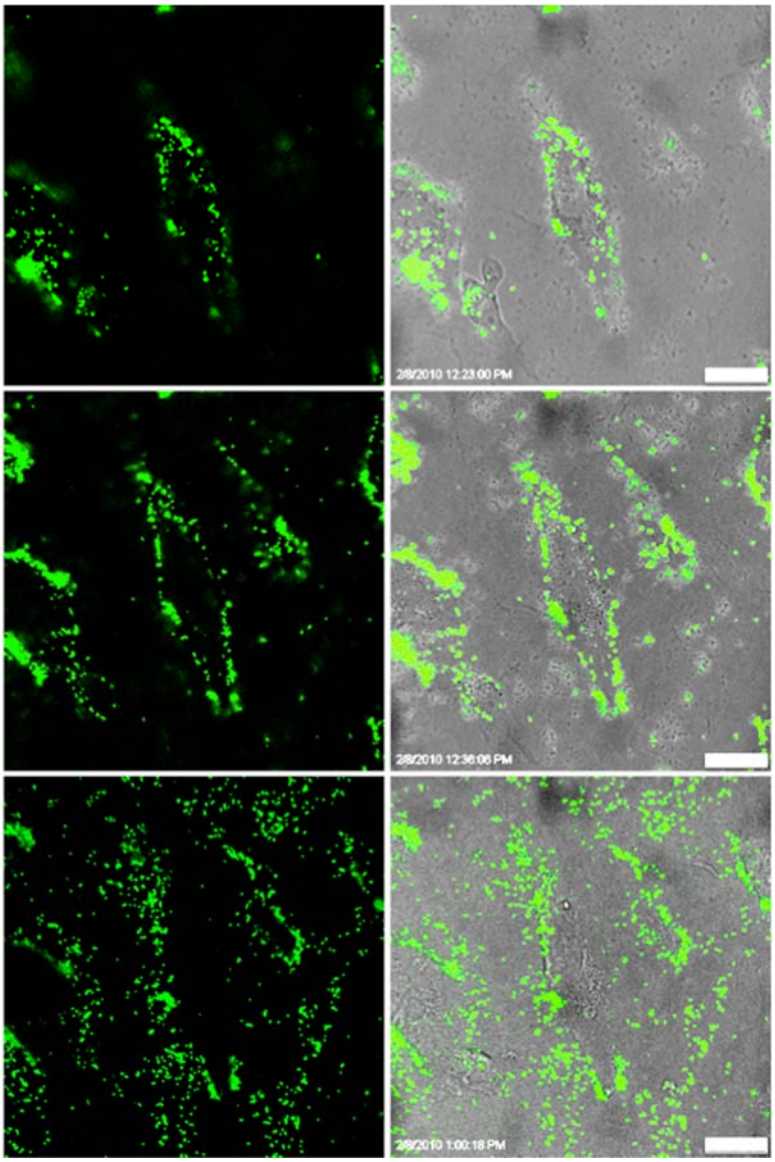

Figure 2. Laser fluorescence confocal micrographs of HUVECs pre-incubated with FITC-MSNs (green spots) after 0 (top), 13 (middle) and 37 (bottom) minutes of addition of fresh growth medium. The images to the left correspond to the FITC channel, and the ones to the right correspond to the overlay of the FITC channel with the corresponding phase contrast images. The images show the migration of the nanoparticles from the interior of the cells to the periphery and eventually to the intercellular space with time. (Scale bar is 25 μm)

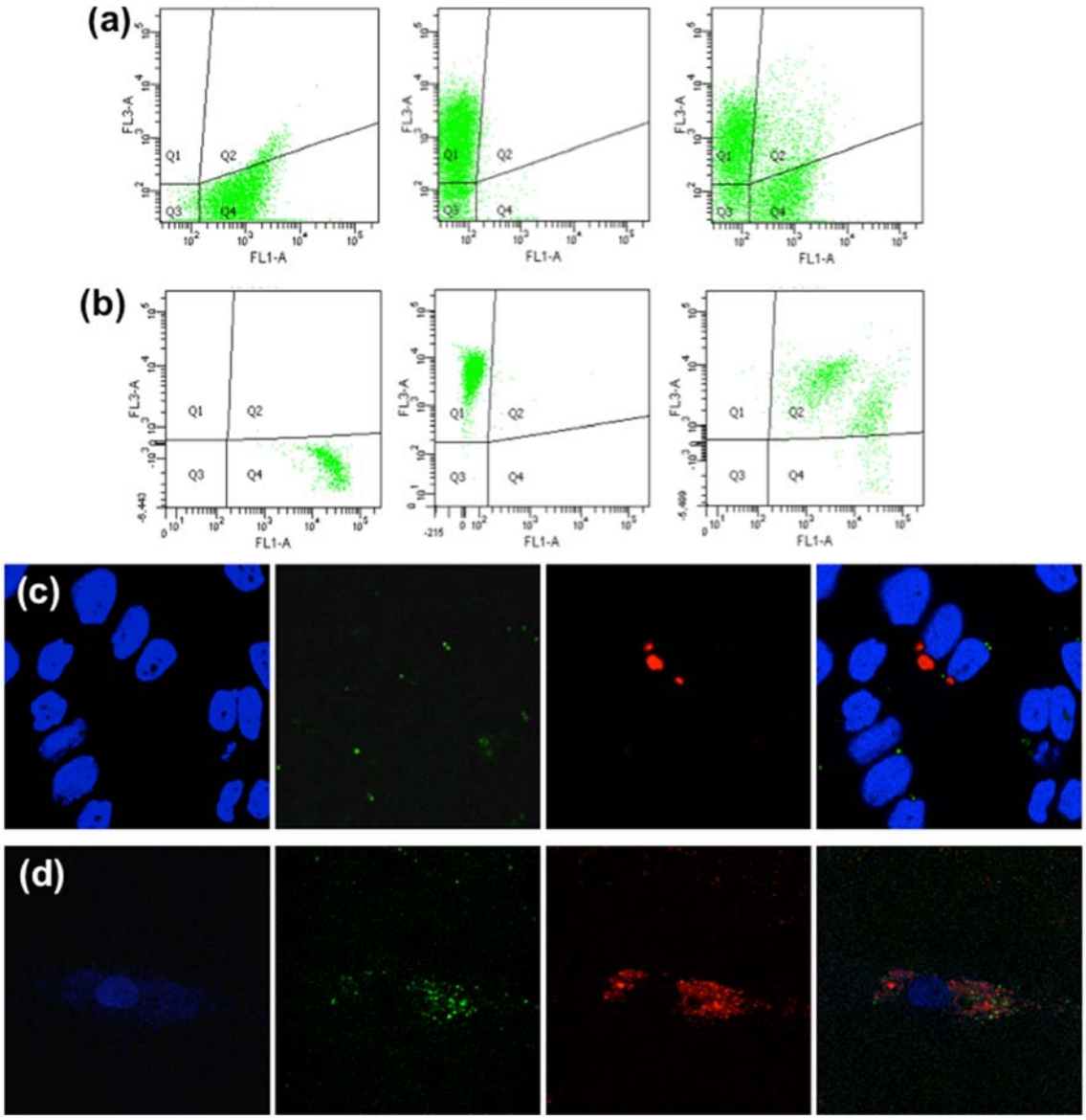

Figure 3. Dot plots from the flow cytometry analysis of the cross-cell experiments using HeLa cells (a) and HUVECs (b). The axes correspond to the intensity of green fluorescence due to uptake of FITC-MSNs (vertical axis) and of red fluorescence due to uptake of TRITC-MSNs (horizontal axis). FITC-fluorescent cells appear in area Q1, TRITC-fluorescent cells in area Q4, and cells with both fluorescent signals appear in area Q2, cells in area Q3 were FITC- and TRITC-negative as determined by a control involving non-labeled cells. Plots at the left correspond to the cells exposed only to FITC-MSNs, center plots correspond to the cells exposed only to TRITC-MSNs, and plots at the right correspond to the co-incubated cells (cross-cell experiment). Confocal fluorescence images of HeLa cells (c) and HUVECs (d) resulting from the cross-cell experiments. The channels from left to right correspond to cell nuclei stained with Hoechst 33258, FITC-MSNs, TRITC-MSNs and the merge of all images.

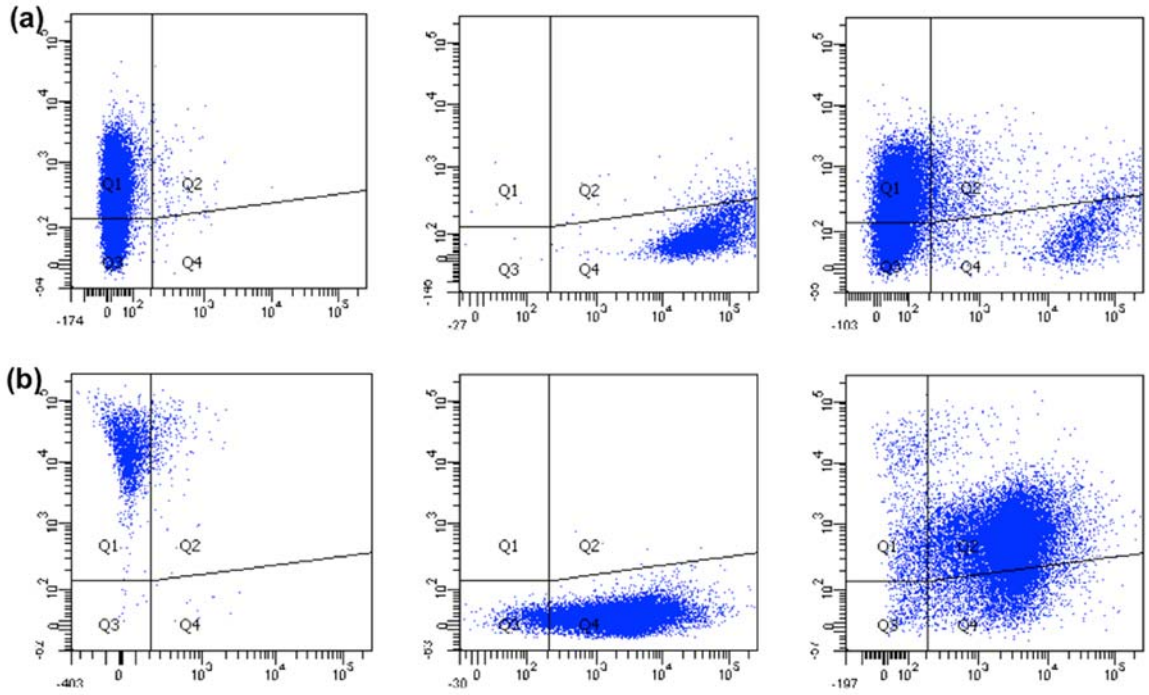

Figure 4. Cross-cell experiments between different cell types. In experiment (a) HUVECs were stained with red fluorescent cell tracer, and HeLa cells were incubated with FITC-MSNs. In experiment (b) HeLa cells were stained with the cell tracer dye and HUVECs were incubated with FITC-MSNs. The vertical axis corresponds to the intensity of green fluorescence due to uptake of FITC-MSNs and the horizontal axis to the intensity of red fluorescence due to dye-labeled cells. Area Q1 corresponds to FITC-fluorescent cells, Q4 to red-labeled cells, Q2 to cells giving both fluorescence signals. Left plots correspond to the cells exposed only to FITC-MSNs, center plots to the red-labeled cells, and the plots to the right to the co-incubated cells (cross-cell experiment). The small proportion of Q2 cells in (a) compared to the large one in (b) suggests an asymmetric nature in the transfer of MSNs between both cell types.

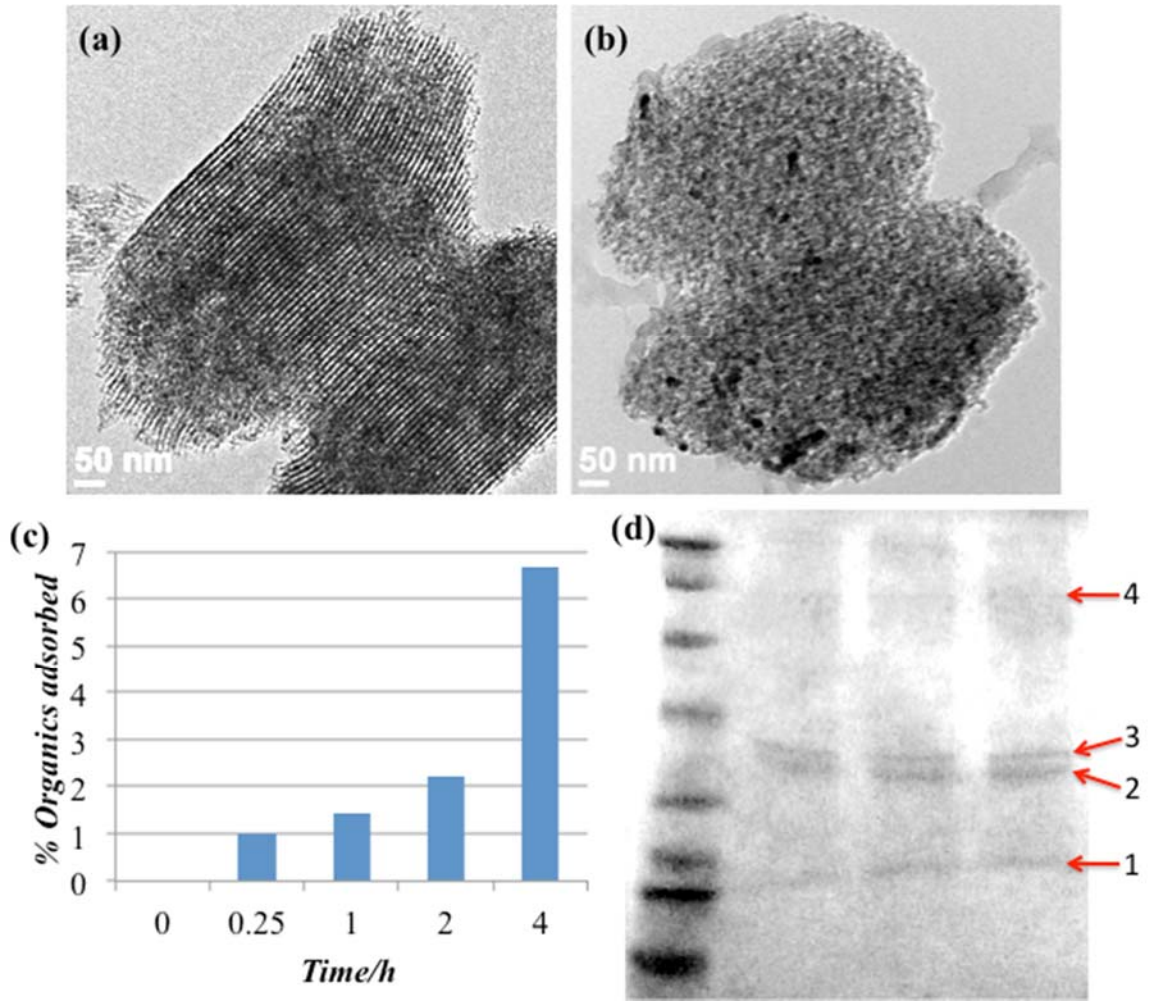

Figure 5. Intracellular protein sequestration by magnetic-MSNs. Transmission electron micrographs of large pored MSNs with superparamagnetic iron oxide nanoparticles embedded in the mesopores. Appearance of the particles before addition (a) and after recovery (b) from the cells. Particle deterioration as well as presence of lower contrast bulks of material suggest capture of organics by the MSNs. (c) Relative amounts of organic species adsorbed to MSNs that were recovered from cell culture, as determined by thermogravimetric analysis. (d) Sodium dodecylsulfate polyacrilamide gel electrophoresis of the extract from the recovered magnetic-MSNs. The first (left) lane is the ladder of molecular weight markers, all the other lanes correspond to the extract from MSNs. The bands indicated by the arrows correspond to the proteins sequestered by the particles, the numbers correspond to the entries in Table 1.

Table 1. Proteins extracted from exocytosed MSNs. The extracted proteins were subjected to MS/MS analysis and the resulting fingerprint spectra were compared to protein databases using Mascot software. Matches with Mowse scores higher than 41 are expected to be identical or highly homologous ($p<0.05$) to the corresponding proteins.

Band	MW	pI	Protein	UniProt Accesion Number	Mowse Score
2	39	7.6	Annexin A2	P07355	55
3	42	5.3	Cytoplasmic actin-1	P60709	290
4	105	5.3	α-Actinin-4	O43707	120